

Slow stable hybrid stars: a new class of compact stars that fulfills all current observational constraints

Germán Lugones^{1,*}, Mauro Mariani^{2,3}, and Ignacio F. Ranea-Sandoval^{2,3}

¹ *Centro de Ciências Naturais e Humanas, Universidade Federal do ABC, Avenida dos Estados 5001, CEP 09210-580, Santo André, SP, Brazil*

² *Grupo de Gravitación, Astrofísica y Cosmología, Facultad de Ciencias Astronómicas y Geofísicas,*

Universidad Nacional de La Plata, Paseo del Bosque S/N, 1900, Argentina and

³ *CONICET, Godoy Cruz 2290, 1425, CABA, Argentina*

(Dated: February 17, 2022)

We study hybrid stars considering the effects on stellar stability of the hadron-quark conversion speed at the sharp interface. The equation of state is constructed by combining a model-agnostic hadronic description with a constant speed of sound model for quark matter. We show that current LIGO/Virgo, NICER, low-density nuclear and high-density perturbative QCD constraints can be satisfied in two scenarios with low and high transition pressures. If the conversion speed is slow, a new class of hybrid objects is possible and very stiff hadronic equations of state cannot be discarded.

I. INTRODUCTION

In spite of several decades of observations and theoretical research, the nature of the deep interior of neutron stars (NSs) is still an unsolved issue. At present, a stringent constraint for the equation of state (EOS) comes from the observed masses of the pulsars PSR J1614-2230 [1], PSR J0348+0432 [2] and PSR J0740+6620 [3], which require that an acceptable EOS must be able to support a NS of at least $2 M_{\odot}$.

New limits on the EOS were posed recently by the LIGO/Virgo detection of gravitational-waves (GWs) coming from the NS-NS merger event GW170817 [4–8]. Assuming that both NSs are described by the same EOS and have spins within the range observed in Galactic binary NSs, the dimensionless tidal deformability $\Lambda_{1.4}$ of a $1.4 M_{\odot}$ NS was found to be in the range 70 – 580 at the 90% level [9]. Also, the fact that the postmerger remnant of GW170817 did not suffer a prompt collapse was used to constrain the maximum gravitational mass of a non-rotating NS ($M_{\max} \approx 2.3 M_{\odot}$) [10]. The mass and radius of the merging objects in the GW190425 event were also inferred, but the possibility that one or both components are black holes cannot be ruled out [11].

Additionally, the Neutron Star Interior Composition Explorer (NICER) has measured the mass and radius of the millisecond-pulsars PSR J0030+0451 [12, 13] and PSR J0740+6620 [14, 15] with great precision. Before the radius measurement of PSR J0740+6620, a comparison of observations with a large variety of EOSs led to the idea that both extremely stiff and soft matter would be ruled out [8, 9]. However, the latest joint NICER and XMM-Newton observation has shown that the inferred radius of PSR J0740+6620 (with $\sim 2 M_{\odot}$) is very similar to that of PSR J0030+0451 (with $\sim 1.4 M_{\odot}$), even though they differ in mass by more than 50% [14, 15].

These results clearly favor stiff EOS models [16] and create some tension with the masses and radii inferred for the objects in GW170817.

For decades, microscopic theories of dense matter have tried to reveal the properties of NS interiors. At present, the EOS is well founded on nuclear theory and nuclear experiments for densities $\lesssim 1 n_0$ (being $n_0 = 0.16 \text{ fm}^{-3}$ the nuclear saturation density). For densities beyond $\sim 40 n_0$, perturbative QCD (pQCD) can describe deconfined quark matter accurately [17, 18], but such large densities are not usually expected in NSs. Between these limits, a robust approach is to use a set of model-agnostic EOSs interpolating both regimes without violating causality, and to require that the resulting NSs configurations fulfill astrophysical constraints. However, it is still unclear at which density would a hadron-quark transition occur and whether hybrid stars (HSs) containing quark cores would exist in Nature.

Concerning HSs, it is under debate whether quarks and hadrons are separated by a sharp discontinuity or by a mixed phase where they coexist along a wide density region forming globally charge-neutral geometrical structures. Mixed phases are energetically preferred if the quark matter surface tension σ is smaller than a critical value σ_{crit} of the order of tens of MeV/fm^2 ; but if $\sigma > \sigma_{\text{crit}}$, the mixed phase is unstable and a sharp interface is favored [19–21]. Unfortunately, calculations of σ give a wide range of values depending on the EOS: the MIT bag EOS gives $\sigma < \sigma_{\text{crit}}$ [22] but $\sigma \gtrsim 100 \text{ MeV}/\text{fm}^2$ is obtained within the Nambu-Jona-Lasinio EOS favoring a sharp interface [23]. Here we will adopt as a working hypothesis that the quark-hadron interface is sharp.

On the other hand, it has been shown that the conversion speed between quarks and hadrons at a sharp interface in a HS is deeply related to the dynamic stability of the object [24–30]. As shown by Chandrasekhar [31], stability can be assessed by inspecting the response of equilibrium configurations to small radial disturbances, since these would grow without bound in an unstable system. However, in the case of HSs, Chandrasekhar’s analysis is

* german.lugones@ufabc.edu.br

not straightforward, since radial perturbations may induce the phase conversion of fluid elements in the neighborhood of the interface. Let us first assume that the conversion timescale τ_{conv} is much larger than the oscillation period τ_{osc} of perturbed fluid elements (*slow* conversions). When a fluid element close to the quark-hadron interface is disturbed and radially displaced from its equilibrium position, it will maintain its chemical composition even if its pressure successively takes values above and below the transition pressure, p_t . Thus, the interface oscillates around its unperturbed position and fluid elements on either side cannot traverse it. Since the interface oscillates with the same period as the disturbances, its movement can be encoded in junction conditions for the relative radial displacement, ξ , and the Lagrangian perturbation of the pressure, Δp , which must be continuous across the phase splitting surface [25]. Otherwise, if conversions are *rapid* ($\tau_{\text{conv}} \ll \tau_{\text{osc}}$), the interface stays at rest with respect to the stellar center and matter can move across it changing *instantaneously* its composition. This implies that $[\xi - \Delta p / (r_t p'_0)]$ and Δp must be continuous across the interface, being r_t its radial position and p'_0 the pressure's radial derivative in the unperturbed configuration [25].

In general, stellar configurations are stable under small radial perturbations if the frequency ω_0 of the fundamental mode verifies $\omega_0^2 \geq 0$ [31]. For cold catalyzed stars, changes of stability ($\omega_0 = 0$) occur at maxima or minima in the $M - \epsilon_c$ diagram, being ϵ_c the energy density at the NS center. Thus, the following static stability criterion holds [32]:

$$\frac{\partial M}{\partial \epsilon_c} < 0 \quad \Rightarrow \quad \omega_0^2 < 0 \quad (\text{unstable star}), \quad (1)$$

$$\frac{\partial M}{\partial \epsilon_c} > 0 \quad \Leftarrow \quad \omega_0^2 \geq 0 \quad (\text{stable star}), \quad (2)$$

However, if perturbed matter is out of thermodynamic equilibrium, changes of stability do not occur necessarily at critical points and Eqs. (1) and (2) may fail [25, 33]. This is the case of HSs with sharp density discontinuities and *slow interface conversions*, where ω_0 can be a real number (indicating stability) even if $\partial M / \partial \epsilon_c < 0$ [24–30, 34]. HSs that are stable even if $\partial M / \partial \epsilon_c < 0$ will be called *slow-stable* (SS) configurations or SS hybrid stars (SSHs). On the contrary, Eqs. (1) and (2) remain valid in HSs with rapid interface conversions since perturbed matter is in thermodynamic equilibrium at all times [25].

In this work, we study HSs focusing on the role of the interface conversion speed on their dynamic stability and taking into account current observational constraints.

II. HYBRID EOS MODEL

For the hadronic crust we use a generalized piecewise polytropic (GPP) fit [35] to the SLy(4) EOS found in Ref. [36] which accurately reproduces the EOS and the adiabatic index. For the hadronic part of the core with

#	Hadronic EOS				Quark EOS		
	$\log_{10} \rho_1$	$\log_{10} \rho_2$	Γ_2	Γ_3	$p_t \left[\frac{\text{MeV}}{\text{fm}^3} \right]$	$\Delta \epsilon \left[\frac{\text{MeV}}{\text{fm}^3} \right]$	c_s^2
1	14.43	14.58	5.9	2.0	150	1800	0.33
2	14.43	14.58	6.2	2.3	150	3000	0.33
3	14.45	14.58	6.5	2.6	150	2000	0.30
4	14.45	14.68	6.5	2.6	70	1000	0.33
5	14.45	14.58	8.5	2.0	20	100	0.50
6					10	100	0.50
7	14.45	14.58	10.0	2.0	60	600	0.20
8					60	900	0.33

TABLE I. Parameters of the selected hybrid EOSs. In all cases we adopted $\log_{10} K_1 = -27.22$ and $\Gamma_1 = 2.764$ for the first polytropic piece of the hadronic core EOS to match the upper limit predicted by cEFT EOSs (see Fig. 1).

baryon number density above $0.3 n_0$ we construct several different model-agnostic GPP EOSs using the prescription of Ref. [35] to ensure continuity in the pressure, the energy density, and the sound speed c_s . The EOS parameters are chosen arbitrarily to obtain ultrastiff EOSs that match at $1.1 n_0$ to the upper limit of a calculated EOS range based on chiral effective field theory (cEFT) interactions including theoretical uncertainties (see Ref. [37] for details). In all cases, causality and consistency with $2 M_\odot$ pulsars are satisfied. Yet, these stiff EOSs are intentionally built to produce *hadronic* M - R curves that do not satisfy the constraints from GW170817 [5, 38].

We assume that at a given pressure, p_t , a first-order phase transition between hadronic and quark matter occurs, with both phases separated by a sharp interface. To keep our analysis as general as possible, quark matter is described by the constant speed of sound model [40], which is parametrized in terms of p_t , the energy density jump $\Delta \epsilon$ between both phases, and c_s (assumed to be constant). The phase transition is described by the Maxwell construction, which guarantees that the pressure and the Gibbs free energy per baryon are the same at both sides of the interface. In this way, we constructed over 3000 hybrid EOSs using combinations of the parameters in the following ranges:

$$10 \text{ MeV}/\text{fm}^3 \leq p_t \leq 300 \text{ MeV}/\text{fm}^3, \quad (3)$$

$$100 \text{ MeV}/\text{fm}^3 \leq \Delta \epsilon \leq 3000 \text{ MeV}/\text{fm}^3, \quad (4)$$

$$0.2 \leq c_s^2 \leq 1, \quad (5)$$

checking consistency with pQCD calculations for $n \gtrsim 40 n_0$ [17, 18] and picking only EOSs whose stellar models verify $2 M_\odot < M_{\text{max}} < 2.3 M_\odot$.

From these results, we selected eight representative hybrid EOS, which are shown in Fig. 1 and detailed in Table I. These EOSs satisfy all recent astrophysical constraints and exemplify qualitatively the broad range of results we obtained.

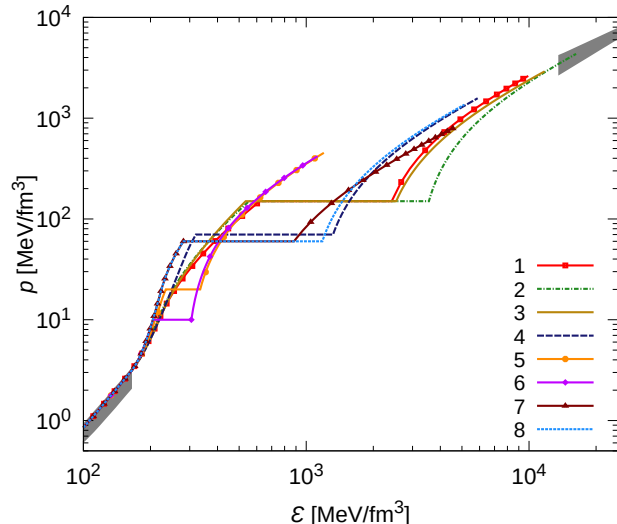


FIG. 1. Selected hybrid EOSs constructed with *stiff* hadronic EOSs ruled out by GW170817 original data analysis but fulfilling NICER and $2 M_{\odot}$ pulsar observations. EOSs are constrained by calculations using cEFT Hamiltonians up to $1.1n_0$ and perturbative QCD results for $n \gtrsim 40n_0$ (gray bands, see Refs. [17, 18, 37]). Curves are displayed up to the largest central density in each HS model. More details of these hybrid EOSs are shown in Table I.

III. RESULTS

In the following, we present our results for the M - R relationship (Fig. 2) and the tidal deformability (Figs. 3 and 4) using the EOSs of Fig. 1. In all figures, we show simultaneously the results for slow and rapid interface conversions. When slow conversions are assumed, all points of the thick curves in Fig. 2 and all points of the curves in Figs. 3 and 4 represent stable configurations. In the rapid case, all HSs with $\partial M/\partial \epsilon_c < 0$ are unstable (i.e. the hybrid branches of models 1-4, 7 and 8).

Our results show that astrophysical constraints are satisfied in two different situations (see Fig. 2):

(a) *Scenario with a low-pressure transition* (models 5 and 6). The main feature of this case is the existence of a long hybrid stellar branch that is stable for both rapid and slow conversions. For this *totally stable* hybrid branch the condition $\partial M/\partial \epsilon_c > 0$ is verified. Observations are not easily fulfilled in this scenario when the PSR J0740+6620 radius is taken into account and *fine tuning* is needed, with low values of p_t and $\Delta\epsilon$.

(b) *Scenario with a high-pressure transition* (models 1-4, 7 and 8). Here, we find a long SS hybrid branch to the left of the maximum mass point in the M - R diagram. Now, astrophysical constraints are fulfilled for a wide range of values of the quark EOS parameters. Twins stars with the same M but different R are possible for a wide range of masses. The baryon number density at the center of SSHSs can be as high as some tens of n_0 (e.g.,

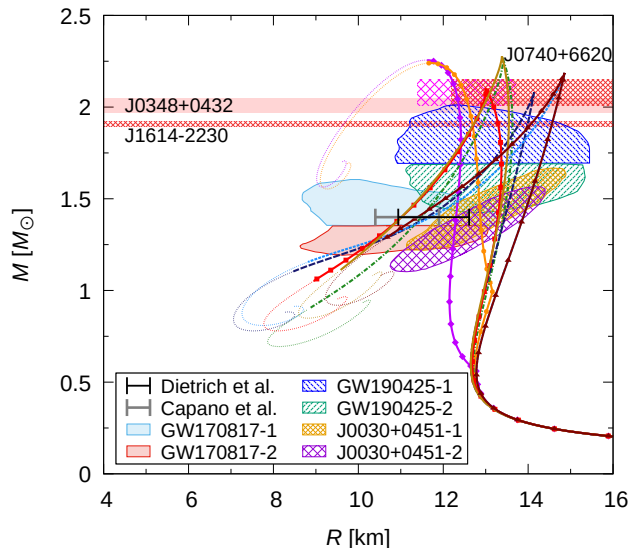


FIG. 2. Mass-radius relationships for the EOSs of Fig. 1 (same color-coding and symbols are used). We also show astrophysical constraints from the $\sim 2 M_{\odot}$ pulsars, GW170817 [5, 7], GW190425 [11], and NICER [12, 13] observations. In gray and black, we show radius constraints from the analysis of Refs. [39] and [8], respectively. When slow conversions are assumed, all points of the thick curves represent stable stars and if conversions are rapid some hybrid segments are unstable (see text). Thin lines represent unstable stars in both scenarios.

our model 2 reaches $66 n_0$ at the center of the last stable object). In this scenario, the stiff hadronic branch fulfills NICER and $2 M_{\odot}$ pulsar constraints, and SSHSs explain GW170817 as well as $2 M_{\odot}$ pulsars and PSR J0740+6620 observations. For a fixed hadronic EOS and a given p_t , we find that the length of the SS hybrid branch depends mostly on $\Delta\epsilon$ and on the stiffness of the quark EOS. Thus, a sufficiently large $\Delta\epsilon$ is needed at the interface in order to explain GW170817.

The dimensionless tidal deformability Λ is shown in Fig. 3 as a function of M . When rapid conversions are assumed, Λ for stable configurations has the standard behavior [42], i.e. the larger the mass the smaller the Λ . However, for slow conversions, Λ can decrease or increase with M meaning that, for a given hybrid EOS, not necessarily the most massive component of a binary NS merger (BNSM) will have the smallest Λ . As for the M - R relationship, the GW170817 constraint is satisfied in the low and in the high pressure interface scenario.

In Fig. 4, we show the Λ_1 - Λ_2 relationship spanning all possible combinations for the masses of the BNSM compatible with the GW170817 event. All BNSMs involving two hadronic stars are outside the 90% confidence contour of GW170817 (label I in Fig. 4), which is an expected result due to our choice of extremely stiff hadronic EOSs. In the case of slow conversions many combinations are in agreement with GW170817: binaries with two SSHSs are inside the 50% region (II), binaries involving a hadronic

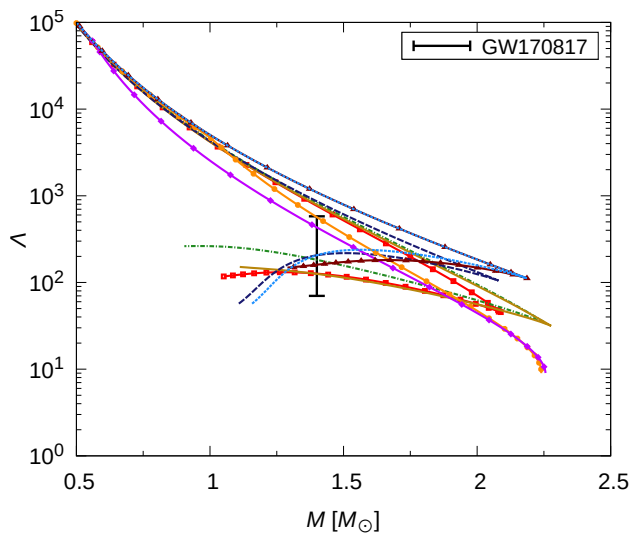


FIG. 3. Dimensionless tidal deformability Λ as a function of the gravitational mass M for the EOSs of Fig. 1 (same colors and symbols are used). In all cases, the hybrid branch fulfills the constraint from the GW170817 event [41] but the hadronic branch does not. For slow conversions, all points of the curves represent stable stars and Λ can be either an increasing or a decreasing function of M . For rapid conversions, the hybrid branches of models 1-4, 7 and 8 are unstable.

star and a SSHS are mostly inside the 90% contour (IIIa and IIIb), and binaries with two totally stable HSs are inside the the 90% region (IV). If rapid conversions are assumed, only binaries involving two totally stable HSs fall inside the 90% confidence contour (IV).

IV. DISCUSSION

In this work we explored new prospects for HS models emerging when the speed of quark-hadron interface conversions is taken into account, and confronted them with current observational constraints.

When rapid interface conversions are assumed, we find that stable HSs compatible with astrophysical observations are possible only if the discontinuity occurs at low enough pressures and the quark EOS parameters are fine-tuned. This occurs because we concentrated intentionally on HSs with extremely stiff hadronic EOSs and on quark EOSs with only one linear piece. Certainly, the use of hadronic EOSs of intermediate stiffness, together with different models of quark matter, will allow other fits to present observational data, albeit less easily than before the NICER measurement of PSR J0740+6620 [38].

On the other hand, our results for HSs with slow interface conversions bring a novel view of the structure of compact stars, which is completely consistent with current astrophysical observations and nuclear/pQCD restrictions. In this picture, purely hadronic NSs made of

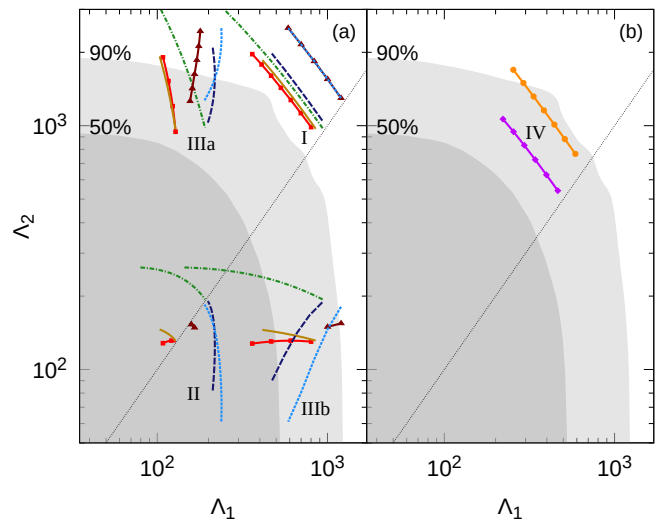


FIG. 4. Tidal deformabilities Λ_1 - Λ_2 for BNSMs with the same chirp mass and mass ratio as GW170817 for the EOSs of Fig. 1 (same colors and symbols are used). Results are split in two panels according to the scenarios described in the text: (a) high-pressure and (b) low-pressure transition. Labels indicate the merging of two hadronic stars (I), two SSHSs (II), a hadronic star with a SSHS (IIIa and IIIb), and two totally stable HSs (IV). In the slow scenario, $\Lambda_1 > \Lambda_2$ is possible because Λ is not necessarily a decreasing function of M .

extremely stiff nuclear matter would have large radii and masses exceeding that of observed $2 M_\odot$ pulsars. To its left in the M - R diagram, there would be a long branch of HSs whose dynamic stability is possible, in spite of $\partial M/\partial \epsilon_c$ being negative, due to the slowness of quark-hadron interface reactions. Our goal in this work has not been to perform an exhaustive analysis of all possible hybrid models that agree with current constraints, but to show that this explanation is feasible and does not require a fine tuning of EOS parameters. Our results also draw attention to the great relevance of microphysical properties such as the surface tension, the curvature energy and reaction timescales, which can completely change our understanding of NS structure but cannot be encoded in $p(\epsilon)$ relationships and derived quantities, no matter how general or comprehensive they may be.

The probable existence of SSHSs opens new interesting scenarios in NS physics and astrophysics. For the hadronic matter EOS, it remarks that stiff and ultra stiff hadronic EOSs are still viable and compatible with current observations. For the quark matter EOS, the possibility of reaching densities tens of times greater than those normally expected in NSs, reinforces the astrophysical significance of studies that explore perturbative QCD in the low-temperature and high-density regime [17, 18, 43]. It also shows that there is not necessarily a tension between astrophysical observations and the theoretically expected conformal limit of the speed of sound

[44, 45]: large observed masses and radii would be explained by hadronic matter with very repulsive contributions and a large sound speed, while the small deformability of GW170817 is naturally explained by a high-pressure first-order phase transition to weakly interacting dense quark matter with $c_s^2 \rightarrow 1/3$. For astrophysics, a new scenario for the existence of two families of NSs is available, together with the standard hybrid star one [40, 46–48] and the proposal of joint existence of hadronic and self-bound strange quark stars [49, 50]. Compared to twin stars already studied in the literature, twins involving SSHSs could span a much wider mass range, between $\sim 1 M_\odot$ to more than $2 M_\odot$. This opens the possibility of catastrophic conversions between stars of both branches with a more significant event rate and may produce extremely energetic transients that could be observed as GRBs, GW bursts, and neutrino emissions.

To conclude, we discuss some features of SSHSs that can help in their observational identification. Certainly, precise mass and radius measurements for a sufficiently large population of sources will significantly reduce the degeneracy of theoretical models and may open up the possibility of identifying SSHS branches if they exist and are long enough. Additionally, future GW detector networks will be able to measure the masses and tidal deformabilities to high accuracy, as well as some quasinor-

mal mode frequencies to within tens of Hz [51]. The tidal deformability of SSHSs is significantly smaller and the f -mode frequency considerably larger [27] than the corresponding values of a hadronic star of the same mass. This characteristic is in agreement with claims that hyper-excited dynamical tides, i.e., anomalously small f -mode frequencies, are disfavored by GW170817 [51]. Moreover, discontinuity g -modes can be excited in SSHSs but don't exist in the case of rapid conversions due to the absence of a buoyancy force [27]. Contrary to g -modes of totally stable HSs which have frequencies below 1 kHz and very long damping times, g -modes of SSHSs have larger frequencies (1 – 2 kHz) and much shorter damping times that facilitate their detection for a given excitation amplitude [27]. This property make SSHSs falsifiable by GW asteroseismology.

ACKNOWLEDGMENTS

G.L. acknowledges the support of the Brazilian agencies CNPq (grant 309767/2017-2) and FAPESP (grant 2013/10559-5). M.M. and I.F.R.-S. thank CONICET and UNLP (Argentina) for financial support under grants PIP-0714 and G157, G007. IFR-S is also partially supported by PICT 2019-0366 from ANPCyT, Argentina.

-
- [1] P. Demorest, T. Pennucci, S. Ransom, M. Roberts, and J. Hessels, Shapiro Delay Measurement of A Two Solar Mass Neutron Star, *Nature* **467**, 1081 (2010), [arXiv:1010.5788 \[astro-ph.HE\]](#).
 - [2] J. Antoniadis *et al.*, A Massive Pulsar in a Compact Relativistic Binary, *Science* **340**, 6131 (2013), [arXiv:1304.6875 \[astro-ph.HE\]](#).
 - [3] H. Cromartie *et al.* (NANOGrav), Relativistic Shapiro delay measurements of an extremely massive millisecond pulsar, *Nature Astron.* **4**, 72 (2019), [arXiv:1904.06759 \[astro-ph.HE\]](#).
 - [4] B. Abbott *et al.* (LIGO Scientific, Virgo), GW170817: Observation of Gravitational Waves from a Binary Neutron Star Inspiral, *Phys. Rev. Lett.* **119**, 161101 (2017), [arXiv:1710.05832 \[gr-qc\]](#).
 - [5] E. Annala, T. Gorda, A. Kurkela, and A. Vuorinen, Gravitational-wave constraints on the neutron-star-matter Equation of State, *Phys. Rev. Lett.* **120**, 172703 (2018), [arXiv:1711.02644 \[astro-ph.HE\]](#).
 - [6] E. R. Most, L. R. Weih, L. Rezzolla, and J. Schaffner-Bielich, New constraints on radii and tidal deformabilities of neutron stars from GW170817, *Phys. Rev. Lett.* **120**, 261103 (2018), [arXiv:1803.00549 \[gr-qc\]](#).
 - [7] C. Raithel, F. Özel, and D. Psaltis, Tidal deformability from GW170817 as a direct probe of the neutron star radius, *Astrophys. J. Lett.* **857**, L23 (2018), [arXiv:1803.07687 \[astro-ph.HE\]](#).
 - [8] C. D. Capano, I. Tews, S. M. Brown, B. Margalit, S. De, S. Kumar, D. A. Brown, B. Krishnan, and S. Reddy, Stringent constraints on neutron-star radii from multimessenger observations and nuclear theory, *Nature Astron.* **4**, 625 (2020), [arXiv:1908.10352 \[astro-ph.HE\]](#).
 - [9] B. Abbott *et al.* (LIGO Scientific, Virgo), GW170817: Measurements of neutron star radii and equation of state, *Phys. Rev. Lett.* **121**, 161101 (2018), [arXiv:1805.11581 \[gr-qc\]](#).
 - [10] L. Rezzolla, E. R. Most, and L. R. Weih, Using gravitational-wave observations and quasi-universal relations to constrain the maximum mass of neutron stars, *The Astrophysical Journal* **852**, L25 (2018).
 - [11] B. P. Abbott *et al.*, GW190425: Observation of a Compact Binary Coalescence with Total Mass $\sim 3.4 M_\odot$, *Astrophys. J. Lett.* **892**, L3 (2020), [arXiv:2001.01761 \[astro-ph.HE\]](#).
 - [12] T. E. Riley *et al.*, A NICER View of PSR J0030+0451: Millisecond Pulsar Parameter Estimation, *Astrophys. J. Lett.* **887**, L21 (2019), [arXiv:1912.05702 \[astro-ph.HE\]](#).
 - [13] M. Miller *et al.*, PSR J0030+0451 Mass and Radius from *NICER* Data and Implications for the Properties of Neutron Star Matter, *Astrophys. J. Lett.* **887**, L24 (2019), [arXiv:1912.05705 \[astro-ph.HE\]](#).
 - [14] T. E. Riley *et al.*, A NICER View of the Massive Pulsar PSR J0740+6620 Informed by Radio Timing and XMM-Newton Spectroscopy, submitted (2021), [arXiv:2105.06980 \[astro-ph.HE\]](#).
 - [15] M. C. Miller *et al.*, The Radius of PSR J0740+6620 from *NICER* and XMM-Newton Data, submitted to *ApJ Letters* (2021), [arXiv:2105.06979 \[astro-ph.HE\]](#).
 - [16] G. Raaijmakers *et al.*, Constraints on the dense matter equation of state and neutron star properties from *NICER*'s mass-radius estimate of PSR J0740+6620 and multimessenger observations, submitted to *ApJ Letters*

- (2021), [arXiv:2105.06981 \[astro-ph.HE\]](#).
- [17] A. Kurkela, P. Romatschke, and A. Vuorinen, Cold Quark Matter, *Phys. Rev. D* **81**, 105021 (2010), [arXiv:0912.1856 \[hep-ph\]](#).
- [18] T. Gorda, A. Kurkela, P. Romatschke, M. Säppi, and A. Vuorinen, Next-to-Next-to-Next-to-Leading Order Pressure of Cold Quark Matter: Leading Logarithm, *Phys. Rev. Lett.* **121**, 202701 (2018), [arXiv:1807.04120 \[hep-ph\]](#).
- [19] D. Voskresensky, M. Yasuhira, and T. Tatsumi, Charge screening at first order phase transitions and hadron quark mixed phase, *Nucl. Phys. A* **723**, 291 (2003), [arXiv:nucl-th/0208067](#).
- [20] T. Endo, Region of hadron-quark mixed phase in hybrid stars, *Phys. Rev. C* **83**, 068801 (2011), [arXiv:1105.2445 \[astro-ph.SR\]](#).
- [21] X. Wu and H. Shen, Nuclear symmetry energy and hadron-quark mixed phase in neutron stars, *Phys. Rev. C* **99**, 065802 (2019), [arXiv:1811.06843 \[nucl-th\]](#).
- [22] M. Berger and R. Jaffe, Radioactivity in strange quark matter, *Phys. Rev. C* **35**, 213 (1987).
- [23] G. Lugones, A. Grunfeld, and M. Al Ajmi, Surface tension and curvature energy of quark matter in the Nambu-Jona-Lasinio model, *Phys. Rev. C* **88**, 045803 (2013), [arXiv:1308.1452 \[hep-ph\]](#).
- [24] C. Vasquez Flores, C. Lenzi, and G. Lugones, Radial pulsations of hybrid neutron stars, *Int. J. Mod. Phys. Conf. Ser.* **18**, 105 (2012).
- [25] J. P. Pereira, C. V. Flores, and G. Lugones, Phase transition effects on the dynamical stability of hybrid neutron stars, *Astrophys. J.* **860**, 12 (2018), [arXiv:1706.09371 \[gr-qc\]](#).
- [26] M. Mariani, M. G. Orsaria, I. F. Ranea-Sandoval, and G. Lugones, Magnetized hybrid stars: effects of slow and rapid phase transitions at the quark-hadron interface, *Mon. Not. Roy. Astron. Soc.* **489**, 4261 (2019), [arXiv:1909.08661 \[astro-ph.HE\]](#).
- [27] L. Tonetto and G. Lugones, Discontinuity gravity modes in hybrid stars: assessing the role of rapid and slow phase conversions, *Phys. Rev. D* **101**, 123029 (2020), [arXiv:2003.01259 \[astro-ph.HE\]](#).
- [28] J. P. Pereira, M. Bejger, L. Tonetto, G. Lugones, P. Haensel, J. L. Zdunik, and M. Sieniawska, Probing elastic quark phases in hybrid stars with radius measurements, *Astrophys. J.* **910**, 145 (2021), [arXiv:2011.06361 \[astro-ph.HE\]](#).
- [29] M. C. Rodríguez, I. F. Ranea-Sandoval, M. Mariani, M. G. Orsaria, G. Malfatti, and O. M. Guilera, Hybrid stars with sequential phase transitions: the emergence of the g_2 mode, *J. Cosmol. Astropart. Phys.* **2021** (2), 009, [arXiv:2009.03769 \[astro-ph.HE\]](#).
- [30] A. Parisi, C. V. Flores, C. H. Lenzi, C.-S. Chen, and G. Lugones, Hybrid stars in the light of the merging event GW170817, to appear in JCAP (2021), [arXiv:2009.14274 \[astro-ph.HE\]](#).
- [31] S. Chandrasekhar, The Dynamical Instability of Gaseous Masses Approaching the Schwarzschild Limit in General Relativity, *Astrophys. J.* **140**, 417 (1964), [Erratum: *Astrophys. J.* **140**, 1342 (1964)].
- [32] B. Harrison, K. Thorne, M. Wakano, and J. Wheeler, *Gravitation Theory and Gravitational Collapse* (University of Chicago Press, 1965).
- [33] E. Gourgoulhon, P. Haensel, and D. Gondek, Maximum mass instability of neutron stars and weak interaction processes in dense matter., *Astron. Astrophys.* **294**, 747 (1995).
- [34] F. Di Clemente, M. Mannarelli, and F. Tonelli, Reliable description of the radial oscillations of compact stars, *Phys. Rev. D* **101**, 103003 (2020).
- [35] M. F. O'Boyle, C. Markakis, N. Stergioulas, and J. S. Read, Parametrized equation of state for neutron star matter with continuous sound speed, *Phys. Rev. D* **102**, 083027 (2020), [arXiv:2008.03342 \[astro-ph.HE\]](#).
- [36] F. Douchin and P. Haensel, A unified equation of state of dense matter and neutron star structure, *Astron. Astrophys.* **380**, 151 (2001), [arXiv:astro-ph/0111092](#).
- [37] K. Hebeler, J. M. Lattimer, C. J. Pethick, and A. Schwenk, Equation of state and neutron star properties constrained by nuclear physics and observation, *Astrophys. J.* **773**, 11 (2013), [arXiv:1303.4662 \[astro-ph.SR\]](#).
- [38] E. Annala, T. Gorda, A. Kurkela, J. Nättilä, and A. Vuorinen, Evidence for quark-matter cores in massive neutron stars, *Nature Physics* **16**, 907 (2020), [arXiv:1903.09121 \[astro-ph.HE\]](#).
- [39] T. Dietrich, M. W. Coughlin, P. T. H. Pang, M. Bulla, J. Heinzel, L. Issa, I. Tews, and S. Antier, Multimesenger constraints on the neutron-star equation of state and the Hubble constant, *Science* **370**, 1450 (2020), [arXiv:2002.11355 \[astro-ph.HE\]](#).
- [40] M. G. Alford, S. Han, and M. Prakash, Generic conditions for stable hybrid stars, *Phys. Rev. D* **88**, 083013 (2013), [arXiv:1302.4732 \[astro-ph.SR\]](#).
- [41] B. Abbott *et al.* (LIGO Scientific, Virgo), Properties of the binary neutron star merger GW170817, *Phys. Rev. X* **9**, 011001 (2019), [arXiv:1805.11579 \[gr-qc\]](#).
- [42] K. Chatziioannou, C.-J. Haster, and A. Zimmerman, Measuring the neutron star tidal deformability with equation-of-state-independent relations and gravitational waves, *Phys. Rev. D* **97**, 104036 (2018), [arXiv:1804.03221 \[gr-qc\]](#).
- [43] A. Kurkela, E. S. Fraga, J. Schaffner-Bielich, and A. Vuorinen, Constraining neutron star matter with Quantum Chromodynamics, *Astrophys. J.* **789**, 127 (2014), [arXiv:1402.6618 \[astro-ph.HE\]](#).
- [44] B. Reed and C. J. Horowitz, Large sound speed in dense matter and the deformability of neutron stars, *Phys. Rev. C* **101**, 045803 (2020), [arXiv:1910.05463 \[astro-ph.HE\]](#).
- [45] P. Bedaque and A. W. Steiner, Sound velocity bound and neutron stars, *Phys. Rev. Lett.* **114**, 031103 (2015), [arXiv:1408.5116 \[nucl-th\]](#).
- [46] S. Benic, D. Blaschke, D. E. Alvarez-Castillo, T. Fischer, and S. Typel, A new quark-hadron hybrid equation of state for astrophysics - I. High-mass twin compact stars, *Astron. Astrophys.* **577**, A40 (2015), [arXiv:1411.2856 \[astro-ph.HE\]](#).
- [47] J.-E. Christian and J. Schaffner-Bielich, Twin Stars and the Stiffness of the Nuclear Equation of State: Ruling Out Strong Phase Transitions below $1.7n_0$ with the New NICER Radius Measurements, *Astrophys. J. Lett.* **894**, L8 (2020), [arXiv:1912.09809 \[astro-ph.HE\]](#).
- [48] M. ShahrbaF, D. Blaschke, A. G. Grunfeld, and H. R. Moshfegh, First-order phase transition from hypernuclear matter to deconfined quark matter obeying new constraints from compact star observations, *Phys. Rev. C* **101**, 025807 (2020), [arXiv:1908.04740 \[nucl-th\]](#).
- [49] I. Bombaci, I. Parenti, and I. Vidana, Quark deconfinement and implications for the radius and the limiting

- mass of compact stars, *Astrophys. J.* **614**, 314 (2004), [arXiv:astro-ph/0402404](#).
- [50] A. Drago, A. Lavagno, G. Pagliara, and D. Pigato, The scenario of two families of compact stars: 1. Equations of state, mass-radius relations and binary systems, *Eur. Phys. J. A* **52**, 40 (2016), [arXiv:1509.02131 \[astro-ph.SR\]](#).
- [51] G. Pratten, P. Schmidt, and T. Hinderer, Gravitational-Wave Asteroseismology with Fundamental Modes from Compact Binary Inspirals, *Nature Commun.* **11**, 2553 (2020), [arXiv:1905.00817 \[gr-qc\]](#).